Robust Pre-Grant Signaling for Energy-Efficient 5G and Beyond Mobile Devices

Soheil Rostami†*, Kari Heiska†, Oleksandr Puchko†, Kari Leppanen†, and Mikko Valkama*

†Huawei Technologies Oy (Finland) Co. Ltd, Helsinki R&D Center
*Department of Electronics and Communications Engineering, Tampere University of Technology
Emails:†{soheil.rostami1, kari.heiska, oleksandr.puchko, kari.leppanen}@huawei.com,
*{soheil.rostami, mikko.e.valkama}@tut.fi

***Abstract*—Mobile device batteries have severely limited capacities, due to constraints on size and weight of mobile devices. Therefore, energy efficiency of mobile devices plays an important role in their usability. Different power measurement studies show that cellular subsystem of mobile device is one of the major contributors to its energy consumption. Thus, reducing energy consumption of cellular subsystem is paramount. In this paper, a new concept of pre-grant message for control plane is introduced, aiming to reduce energy consumption of cellular subsystem in downlink, while discontinuous reception is activated. Performance of the proposed scheme in terms of false alarm and misdetection are investigated, and evaluated in AWGN and Rayleigh fading channel. The obtained numerical results show that such a signaling can reduce power consumption of mobile device by up to 70% for bursty data applications, at the cost of negligible increments in signaling overhead.**

***Index Terms*—energy efficiency, mobile device, DRX, LTE, 5G.**

I. Introduction

Fifth generation mobile networks, also known as 5G, are expected to provide high data rates and reduced latency to users in order to deliver diverse set of new services such as ultra-high-definition video streaming or augmented reality [1]. To satisfy the aggressive requirements of such services, advanced physical layer techniques are vital; leading to increased computational complexity and high power consumption of the mobile device.

Despite mobile devices have become faster and powerful, their batteries still last less than a day under moderate use, making battery life a perennial problem for mobile phone owners. Furthermore, according to a survey by Qualcomm, 60% of the consumers stated that battery life performance is the major attribute that they wanted to be improved [2]. This issue can be solved either by increasing energy density of batteries or by reducing the power consumption. However, mobile devices energy density (which is battery capacity divided by mobile phone screen area) has increased just a few percent during the last decade [3]. In other words, the battery evolution lags far behind changes in semiconductor industry.

Modern smartphones have multiple subsystems such as wireless connectivity, an application processor, a graphic processor, an Audio codec, and human interfaces. Multiple detailed analyses of energy consumption of commercial smartphones, under moderate use show that display, application processor, and cellular subsystem are the main consumers of energy for mobile phones, and the other components contribute substantially only when they are used intensively [2], [4], [5]. Energy consumption of display and application processor are out of scope of this paper, and therefore we mainly focus on the cellular subsystem.

The cellular subsystem consists of transmitter, receiver, and interface towards the rest of the terminal. Despite the fact that the transmitter has considerably higher power consumption, it is important to reduce energy consumption of mobile device in receive mode too; the main reason is that most of time cellular subsystem operates in receive mode, and its energy consumption can accumulate during a day, and eventually surpasses transmit energy consumption.

3rd generation partnership project (3GPP) specified discontinuous reception (DRX), as a promising solution for enhanced battery life by means of switching off RF circuitry and other modules for long periods, activating it only for short intervals. In spite of using DRX in long-term evolution (LTE), an LTE cellular subsystem is about 23 times less power efficient in comparison to WiFi, and even worse compared to 3G systems [6]. In other words, DRX as used in LTE still needs to be improved.

The main contribution of this paper is to introduce a novel narrow-band control plane signaling method, referred to as pre-grant message (PGM), in order to improve energy efficiency of mobile devices, while DRX is activated. In the proposed approach, a mobile device listens to PGM at the beginning of its DRX cycle. The introduced scheme is adapted for the LTE frame structure, and can easily be generalized to any other emerging 5G frame structures.

In this work, vectors are denoted by bold letters, e.g. $\mathbf{H}_x$, and their elements are shown by superscript, for instance $H_x^{(m)}$ refers to m^{th} element of $\mathbf{H}_x$. In addition, $\circ$ and * denote Hadamard product and complex conjugate respectively.

This paper is organized as follows. Section II describes the reasons behind energy inefficiency of the DRX-mechanism, which needs to be addressed. Further, the proposed solution to improve energy efficiency of DRX is explained in Section III. Signaling structure of PGM, analytical analysis of detection and false alarm rates, as well as description of PGM receiver are discussed in Sections IV, V and VI, respectively. These are

This work has received funding from the European Union's Horizon 2020 research and innovation program under the Marie Skłodowska-Curie grant agreement No. 675891 (SCAVENGE), and Tekes TAKE-5 project.

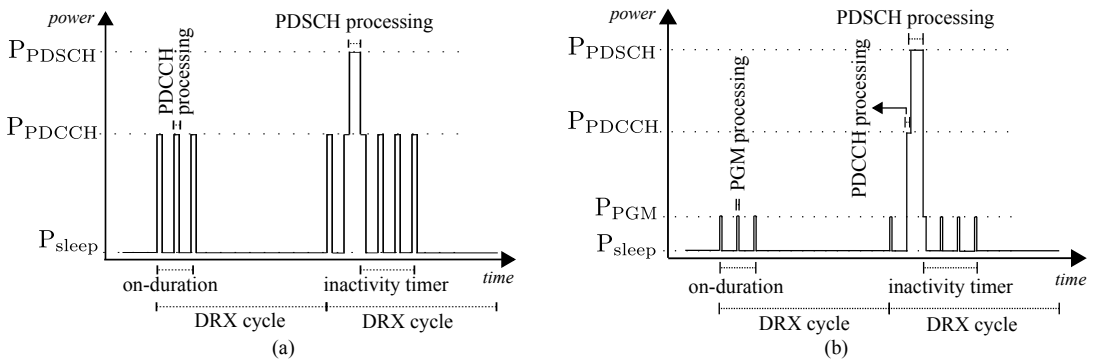

Fig. 1. Power consumption of cellular subsystem under, (a) DRX mechanism, and (b) the proposed mechanism.

followed by simulation results and conclusion in Sections VII and VIII, respectively.

II. Problem Description

5G is envisioned to provide significantly higher data rates, and lower latency compared to LTE [1]. Therefore, high channel bandwidth for data transfer is imperative; however, high bandwidth communication can exhaust the mobile devices battery power quickly. It is anticipated that 5G in some use cases may require bandwidths up to 400 MHz [5].

Moreover, similar to LTE, 5G is an all-IP network, in which mobile users frequently have bursty traffic, with occasional periods of transmission activity followed by longer periods of silence. In respect to latency requirements, it is beneficial to scan physical downlink control channel (PDCCH) in each subframe to receive downlink (DL) data traffic or uplink grants, and promptly make an appropriate reaction to the PDCCH [7]. Depending on number of active users and available bandwidth, PDCCH can occupy different number of resource elements, ranging from one to four OFDM symbols per subframe. Higher dimension of PDCCH can impact mobile battery life time.

The DRX-enabled mobile device monitors the PDCCH only in a fraction of each subframe within on-duration period of a DRX cycle, and then switches off some components of cellular subsystem in the remaining subframes. The main parameters required for the sleep/wake scheduling of each terminal are on-duration timer, inactivity timer and DRX cycle. The aforementioned timers have a significant impact on the achievable energy savings and the delay incurred by the mobile device applications [8].

The average power (P_l) consumed by cellular subsystem in receive mode during a DRX cycle can be modeled as follows

$$P_l = \frac{T_{PDCCH}P_{PDCCH} + T_{PDSCH}P_{PDSCH}}{T_{PDCCH} + T_{PDSCH}}, \quad (1)$$

where P_{PDCCH} is power required to monitor PDCCH for average duration of T_{PDCCH}; P_{PDSCH} is required power of cellular subsystem for decoding physical downlink shared channel (PDSCH) for average duration of T_{PDSCH}. Further, T_{PDCCH} consists of average time duration (T_{uf}) that cellular subsystem decodes PDCCH, leading to data reception, and average time duration (T_{ul}) that does not end to any data reception.

According to experimental findings on actual mobile devices available in market, the time period that mobile devices monitor PDCCH without any data allocation has a major impact on battery consumption [3]. In other words, the main issue with DRX, is high wasted energy consumption ($T_{ul}P_{PDCCH}$) of mobile device during PDCCH decoding, while it does not contain any DL data traffic or uplink grants; this issue can become severe for 5G, due to need for high bandwidth communication.

III. Proposed Solution: Pre-Grant Message

Reducing energy consumption of empty DRX cycles, has a significant potential to expand the battery life time of mobile devices. This can be achieved either by reducing T_{ul} or P_{PDCCH}. The former is an inevitable part of DRX mechanism, and it can be optimized by assigning different DRX configurations per radio bearer [8]. The latter can be realized by re-designing PDCCH in such a way that it requires less energy to decode it. However, it would require considerable modifications in the existing standard.

In the proposed method, mobile device energy consumption is reduced by transmitting a new narrow-band signal, PGM, one subframe in advance. PGM informs of potential scheduling on next subframe's PDCCH or rather if it can skip next subframe's PDCCH. Because of signal structure of PGM, described in detail in the next section, the required energy to decode it, is less than PDCCH processing.

Power consumption of DRX-enabled cellular subsystem and the proposed method are illustrated intuitively in Fig. 1(a) and Fig. 1(b), respectively. Assume that network has data for the mobile device on second subframe of second DRX cycle. As shown in Fig. 1(a), in case of conventional DRX-enabled cellular subsystem, the mobile device checks PDCCH every subframe during on-duration and inactivity timers, and eventually in second subframe of second DRX cycle, it realizes that there is upcoming data. However in the proposed mechanism, the mobile device checks the PGM every subframe of on-duration and inactivity timers. As shown in Fig. 1(b), the mobile device knows from decoding PGM in first subframe of first DRX cycle that there is no grant for

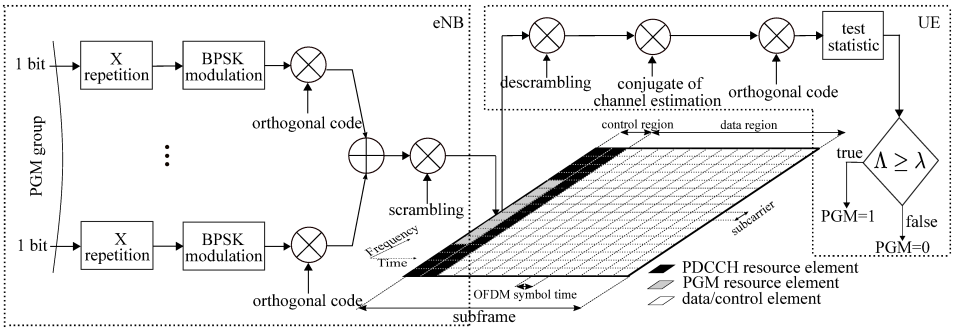

Fig. 2. PGM generation at eNB, PGM processor in UE side, and LTE time-frequency grid illustrating PGM signal structure

second subframe; therefore during second subframe of first DRX cycle, the cellular subsystem only needs to decode PGM. In the second DRX cycle, decoded PGM in first subframe indicates that there is scheduling data for second subframe, thus the cellular subsystem starts processing PDCCH in second subframe, in order to receive PDSCH.

The average power consumption (P_2) of PGM-enabled cellular subsystem during a DRX cycle can be calculated as follows

$$P_2 = \frac{T_{PGM}P_{PGM} + T'_{PDCCH}P_{PDCCH} + T_{PDSCH}P_{PDSCH}}{T_{PGM} + T'_{PDCCH} + T_{PDSCH}}, \quad (2)$$

where T_{PGM} is time duration of PGM processing, and P_{PGM} is power consumption required for processing of PGM, which is much less than P_{PDCCH}; additionally, $T'_{PDCCH} = T_{uf}$. The main reasons for $P_{PGM} << P_{PDCCH}$ is that PGM has very narrow-band signal structure, and contains very little data to process, while PDCCH can have high dimension especially when the number of users is high. Secondly, PGM is spread during one OFDM symbol, while PDCCH can range from one to four OFDM symbols, therefore it increases energy consumption of cellular subsystem. In this work, we assume that the PDCCH occupies the first two OFDM symbols at the beginning of each subframe, as shown in Fig. 2.

For comparison purposes, we define a relative power saving parameter, referred to as $\eta = \frac{P_1 - P_2}{P_1}$. The value of η ranges form 0 to 1, and greater η indicates that the mobile device using the proposed mechanism conserves energy much better than ordinary DRX-enabled cellular subsystem.

IV. Pre-Grant Message Signal Structure

By enabling PGM, each mobile device decodes pre-assigned and pre-reported search space (in frequency and time domains), in order to decide whether it needs to check the PDCCH in next subframe (PGM=1) or not (PGM=0). For this purpose, a structure, where several PGMs are code multiplexed onto a set of continuous subcarriers, during one OFDM symbol, is applied.

PGM requires to have very low detection error rates. For this purpose, PGM needs to have power control mechanism as a function of radio environments; the allocated power for m^{th} code is represented by P_m. However, due to RF power dynamic range restrictions, the desired powers may not be met, especially for cell-edge users. Therefore, each PGM can be spread on multiple resource elements to reduce the power differences while at the same time providing the energy necessary for accurate reception.

The PGM (single bit of control information per mobile device) is repeated X times, followed by BPSK modulation and spreading with a length-M orthogonal sequence, referred to as $\mathbf{q}_m$ with dimension of M; because of orthogonality among codes, $\sum_{m=1}^{M} q_r^{(m)} q_f^{(m)}$ equals 0, if $f \neq r$ or equals M, if $f = r$.

We refer to a set of $2M$ PGMs transmitted on the same set of $X \times M$ subcarriers, as a PGM group. Thus, an individual mobile device can be assigned by a single number (between 1 to $2M$), representing the index of the assigned orthogonal sequence within the group. The first set of M orthogonal codes are formed by $M \times M$ Hadamard matrix, and the second set of M codes are in quadrature ($\times j$) to the first set.

After multiplexing the signal representing the PGMs in a group, cell-specific scrambling is applied, which makes neighboring cell interference appear as uncorrelated noise in user equipment (UE) side. Fig. 2 depicts the signal structure of the PGM, PGM generation at eNB, and PGM processor in UE side. For presentation simplicity, other components such as the cyclic prefix remover/adder, FFT/IFFT are not shown.

The introduction of PGM can cause misdetection and false alarm. In latter case, mobile device erroneously identifies 0 as 1 for its decoded PGM, leading to unnecessary power consumption of cellular subsystem, thus the false alarm is required to be minimized. The former corresponds to the case, where UE decodes PGM as 0 incorrectly, while 1 was sent. The misdetection can add an extra delay, and waste capacity in both PDCCH and PDSCH. Therefore, the misdetection rate requirement of PGM is eventually stricter than false alarm rate.

Configuration parameters of PGM are part of system information, and can be transmitted on the broadcast channel; it contains bits indicating the location of subcarriers, the scrambling code, and the index number of orthogonal code as well as DRX-related configurations.

V. System Model and Detection Error Rates

The samples of the received baseband OFDM signal of PGM, after removing cyclic prefix, demodulating by FFT,

followed by descrambling with assumption of an ideal synchronization can be represented as a vector $\mathbf{Y}_x$ with dimension of M for $x \in \{1, ..., X\}$, expressed as

$$\mathbf{Y}_x = \mathbf{H}_x(\sum_{m=1}^{M} \sqrt{\frac{P_m}{2}} i_m \mathbf{q}_m + j \sum_{m=1}^{M} \sqrt{\frac{P_m^{'}}{2}} i_m^{'} \mathbf{q}_m) + \mathbf{W}_x, \quad (3)$$

where $i_m \in \{-1, +1\}$ for $m \in \{1, ..., M\}$ is a BPSK modulated symbol of PGM belonging to m^{th} mobile device in the group; similarly, $i_m^{'}$ is a BPSK symbol, for $(m+M)^{th}$ mobile device in the group. Also, $\mathbf{H}_x$ is an M-dimensional complex vector of frequency response; P_m and $P_m^{'}$ are the power levels of m^{th} orthogonal code and quadrature of m^{th} orthogonal code, respectively. Finally, we assume that noise comes from an additive white Gaussian noise (AWGN) process, and can be represented as a circularly symmetric zero-mean complex Gaussian, referred to as an M-dimensional complex vector $\mathbf{W}_x$, with covariance matrix of $\sigma_w^2 I$. Without loss of generality, the following analyses in this section are performed from first ($m = 1$) mobile device perspective.

The likelihood function for decoding PGM can be modeled as the following test statistic

$$\Lambda = \mathfrak{Re}\Big(\sum_{x=1}^{X} \sum_{m=1}^{M} q_1^{(m)} (\mathbf{Y}_x \circ \hat{\mathbf{H}}_x^{*})^{(m)} \Big), \quad (4)$$

where $\hat{\mathbf{H}}_x$ is channel estimate for coherent detection, and is acquired based on either cell-specific reference signals or demodulation reference signals. Channel estimate can be written as $\hat{\mathbf{H}}_x = \mathbf{H}_x + \mathbf{e}_x$, where $\mathbf{e}_x$ is the estimation error. In this paper, channel is represented as a Gaussian process, therefore estimation error can be modeled as circularly symmetric zero mean Gaussian with covariance $\sigma_e^2 I$ [9], [10].

In this work, a statistical hypothesis testing is utilized to decide whether to accept $\mathcal{H}_0$ or $\mathcal{H}_1$. The null hypothesis $\mathcal{H}_0$ is a claim that the value of a transmitted PGM equals 0, while the alternate hypothesis $\mathcal{H}_1$ is a claim opposite to $\mathcal{H}_0$, stating that PGM is 1. The mobile device compares calculated value of Λ from (4) with a fixed detection threshold λ, and then decides whether PGM is zero or one (Fig. 2).

By substituting (3) into (4), and skipping irrelevant multiplicative and additive terms, Λ can be expressed as

$$\Lambda = \sum_{x=1}^{X} \sum_{m=1}^{M} |H_x^{(m)}|^2 \sqrt{\frac{P_1}{2}} i_1 +$$

$$\mathfrak{Re}\Big(\sum_{x=1}^{X} \sum_{m=1}^{M} {H_x^{(m)}}^* W_x^{(m)} \Big) + \mathfrak{Re}\Big(\sum_{x=1}^{X} \sum_{m=1}^{M} {e_x^{(m)}}^* W_x^{(m)} \Big) +$$

$$\mathfrak{Re}\Big(\sum_{x=1}^{X} \sum_{m=1}^{M} H_x^{(m)} {e_x^{(m)}}^* \Big) \sqrt{\frac{P_1}{2}} i_1 -$$

$$\mathfrak{Im}\Big(\sum_{x=1}^{X} \sum_{m=1}^{M} H_x^{(m)} {e_x^{(m)}}^* \Big) \sqrt{\frac{P_1^{'}}{2}} i_1^{'} \quad (5)$$

In case of error-free channel estimation or equivalently $\mathbf{e}_x = \mathbf{0}$, Λ would have only signal and noise parts (first and second terms), however due to presence of estimation errors, various undesirable effects crop up in the course of calculating the Λ. Such imperfections consist of self-interference (fourth term), co-channel interference (fifth term), and extra noise (third term). When such imperfections are superimposed on the test statistic, the average loss in SNR is inevitable.

If the channel is AWGN, Λ contains the effects of the noise and the equal attenuation of the signal magnitude for subcarriers, i.e. $H_x^{(m)} = h$; SNR for AWGN, referred to as β^{AWGN}, can be calculated as follows

$$\beta_{AWGN} = \frac{XMP_1|h|^4}{\sigma_e^2 \sigma_w^2 + \sigma_w^2 |h|^2 + 0.5\sigma_e^2 (P_1 + P_1^{'})|h|^2}. \quad (6)$$

As can be seen on above equation, repeating PGM (X-times), spreading data (with length of M), and power control (P_m) can increase SNR with gain of $X \times M \times P_m$. Increasing the gain can reduce both probability of false alarm (P_{fa}) and misdetection (P_{md}) over fading channels.

P_{fa} is the probability of deciding to monitor PDCCH, while $\mathcal{H}_0$ is true, i.e, $P_{fa} = \Pr(\Lambda \geq \lambda | \mathcal{H}_0)$. P_{md} is the probability of deciding to not monitor PDCCH, while $\mathcal{H}_1$ is true, i.e. $P_{md} = \Pr(\Lambda < \lambda | \mathcal{H}_1)$. As explained in Section II, based on different measurements, frequency of occurrence of $\mathcal{H}_0$ is much higher than $\mathcal{H}_1$, i.e. $\Pr(\mathcal{H}_0) >> \Pr(\mathcal{H}_1)$.

By denoting A as an inter distance between means of $\mathcal{H}_0$ and $\mathcal{H}_1$ in case of error-free channel estimation, A can be shown to equal $2\sqrt{|h|^2 XMP_1}$; the aforementioned conditional probabilities under AWGN assumption can then be written as follows [11]

$$P_{fa,AWGN} = Q(\frac{A + 2\lambda}{2\sigma_w}), \quad (7)$$

and

$$P_{md,AWGN} = Q(\frac{A - 2\lambda}{2\sigma_w}), \quad (8)$$

where Q is the Q-function representing the tail probability of the standard Gaussian distribution.

Intuitively, detection threshold λ should be set at some intermediate level, $(-A/2 \leq \lambda \leq +A/2)$. The threshold has a direct impact on detection error rate. An error in a conventional digital communication system, is an error, regardless of its more specific type (0 to 1 or 1 to 0); however, PGM needs to have asymmetric error rates with considerably smaller P_{md} compared to P_{fa}. Hence, λ should be adjusted to satisfy the average error probability of detection and false alarms.

Without loss of generality, we can assume that threshold level is denoted by $\lambda = \frac{A}{2}\nu$, with $-1 \leq \nu \leq 1$. Thus (7) and (8) can be simplified as

$$P_{fa,AWGN} = Q((1+\nu)\sqrt{2\beta_{AWGN}}), \quad (9)$$

and

$$P_{md,AWGN} = Q((1-\nu)\sqrt{2\beta_{AWGN}}). \quad (10)$$

Both probabilities in a slow Rayleigh fading channel can then be evaluated by averaging over channel realizations [11]

$$P = \int_0^{\infty} P_{AWGN}(\beta) P_{df}(\beta) d\beta, \quad (11)$$

where $P_{AWGN}(\beta)$ is either $P_{fa,AWGN}$ or $P_{md,AWGN}$ as functions of SNR β; $P_{df}(\beta)$ is the probability density function of β, which is a Chi-squared distribution. Ultimately, result of both integrals can be expressed as follows

$$P_{fa} = \frac{1}{2}\big(1 - \sqrt{\frac{\overline{\beta}}{\frac{1}{(1+\nu)^2} + \overline{\beta}}}\big), \tag{12}$$

and

$$P_{md} = \frac{1}{2}\big(1 - \sqrt{\frac{\overline{\beta}}{\frac{1}{(1-\nu)^2} + \overline{\beta}}}\big), \tag{13}$$

where $\overline{\beta}$ is average of SNR β over different channel realizations.

Reliability and energy efficiency are essential characteristics of PGM, thus a low P_{fa} and an even lower P_{md} are preferred. The operating point of the PGM can be specified by the network operator. In this work, error rates of P_{fa} and P_{md} of the order of 10% and 1%, respectively are targeted. The target unequal error protections ($P_{fa} < 10\%$ and $P_{md} < 1\%$) can be achieved by configuring processing gain ($X \times M$), P_m at eNB, as well as ν in terminal side.

VI. Pre-Grant Message Processor

As shown in Fig. 2, the received signal is first descrambled and demapped from $X \times M$ resource elements in the time-frequency grid. Both processes retrieve back the $X \times M$ symbols in order. The resultant symbols $\mathbf{Y}_x$ are multiplied with the estimated value of conjugate of the complex channel frequency response vector $\hat{\mathbf{H}}_x^*$, element by element. Then the result $((\mathbf{Y}_x \circ \hat{\mathbf{H}}_x^*))$ undergoes inner product with the $\mathbf{q}_1$ sequence. Then sum of inner products $(\sum_{m=1}^{M} q_1^{(m)}(\mathbf{Y}_x \circ \hat{\mathbf{H}}_x^*)^{(m)})$ over x are calculated as part of test statistic. For all the elements the multiplication is performed, and the results are accumulated as a 64 bit value. The real part of the accumulated value alone is taken, which is a 32 bit value. Finally by comparing to pre-set threshold, mobile device can estimate the one-bit PGM.

For demonstration purposes, the PGM processor can be designed and implemented on a FPGA. In this work, power consumption of the realization of architecture for the PGM processor on Xilinx Spartan 3E family, is estimated using Xilinx power estimator tool. According to the pre-design estimation, it can consume up to 60 mW dynamic power, when the processing gain is 4×8. Its required clock can be shared from the main baseband unit of cellular subsystem.

The device utilization summary for the proposed PGM processor is provided in Table I. Further, the power consumption of PGM processor can be reduced about 7-14 times using application-specific integrated circuits (ASIC) [12].

VII. Example Numerical Results

In this section, a set of link-level simulation results are provided to validate the concept and analytical results, as well as to show and compare the energy efficiency of PGM over solely DRX-enabled mobile devices.

TABLE I
Estimation of FPGA resource utilization (numbers of specific blocks) for PGM processor

flip flops	adders	multipliers	LUT	P_{PGM}
≤ 600	≤ 400	≤ 100	≤ 700	≤ 60 mW

TABLE II
Assumed power consumption parameters

P_{PDSCH}	P_{PDCCH}	P_{PGM}	P_{sleep}
500 mW	255.5 mW	60 mW	11 mW

Simulations are performed in an urban area, where the cell radius is 500 m, and is operating on 900 MHz carrier frequency; additionally, UEs are randomly distributed with uniform distribution within a single cell which has 16 ($2 \times M$) DRX-activated UEs using $M = 8$-length orthogonal codes, and each PGM is repeated four times ($X = 4$). Furthermore, each simulation scenario lasts for $10,000$ TTIs, and is repeated 100 times for averaging results. The multipath intensity profile of the Pedestrian-A channel is considered; additionally, error vector magnitude ($100 \times \sqrt{\sigma_e{}^2/P_{ref}}$) of 5% is assumed stemming from the reference signal based channel estimation errors. We also assume that allocated powers P_m for all users, $m \in \{1, ..., M\}$ are identical.

Energy consumption of mobile device in different operating states (sleep, PGM, PDCCH, and PDSCH processing) is highly dependent on the mobile device implementation and also its operational configurations. Therefore, for preliminary numerical results, the power consumption model used in [13], [14] is utilized; its parameters are shown in Table II. Fig. 3 and Fig. 4 illustrate the PGM performance in terms of false alarm and misdetection rates for two different values of the repetition code length X at different threshold levels. As it can be seen, lowering the ν or equivalently λ reduces P_{md} and simultaneously increases P_{fa}. Raising ν has the opposite effect. Furthermore, X as a factor of processing gain plays an important role, and easily both figures depict that increasing X can reduce both error probabilities, resulting on improvement in both reliability and energy efficiency.

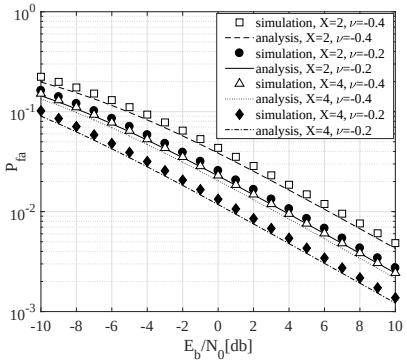

Fig. 3. P_{fa} as a function of SNR per bit with spreading code length of 8.

Moreover, both figures show that the proposed mechanism is robust for low SNR regions, such as cell edges. For very severe SNRs per bit (E_b/N_0) such as -10 dB, using $\nu = -0.4$

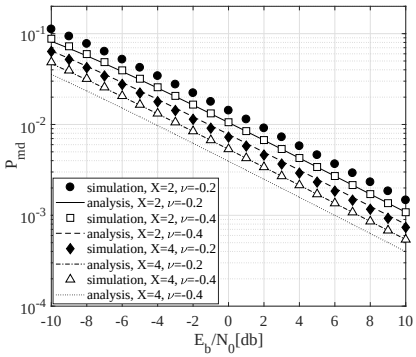

Fig. 4. P_{md} as a function of SNR per bit with spreading code length of 8.

and $X = 4$, the proposed method has 15.1% false alarm rate and 4.8% misdetection. However, for reasonable SNR range, e.g. 0 dB, PGM has $P_{fa} = 2.3\%$ and $P_{md} = 0.53\%$ using $\nu = -0.4$ and $X = 4$, which satisfies both asymmetric error rate requirements, i.e. $P_{fa} < 10\%$ and $P_{md} < 1\%$.

As mentioned in Section V, due to the existence of channel estimation errors, there is SNR loss, which can degrade the performance of PGM detection; both Fig. 3 and Fig. 4 show that channel estimation errors deteriorate P_{fa} and P_{md}. In our simulations, we assumed that there is additional error vector magnitude of 5%, stemming from channel estimation errors, leading to some difference between analytical and simulation results. Both figures indicate that the differences between the analytical and simulation results are, however, very small, and thus it is clear that the theoretical analysis is consistent with the simulation results.

To next investigate the impact on power consumption of mobile device, the power saving parameter η for different DRX configurations under different traffic types are summarized in Table III. DRX parameters are assigned with typical values for the corresponding traffic type [8], [15]; as it is shown, for better SNR environments, due to fact that P_{fa} and P_{md} are very low, regardless of traffic type, achievable power savings are large. However, even in case of poor SNR (-10 dB), η in the worst case scenario is 42%.

Furthermore, type of traffic has a direct impact on the performance of PGM. The main reason is that DRX parameters are optimized per traffic, which leads to different on-duration and inactivity timers. In case of bursty data, the averages of both timers are higher than with video and VoIP, leading to larger power saving. Finally, $\Pr(\mathcal{H}_0)$ impacts the energy efficiency of PGM over solely DRX-enabled scenario. $\Pr(\mathcal{H}_0)$ depends on traffic type and DRX configurations, namely for higher $\Pr(\mathcal{H}_0)$, PGM can reduce power consumption much more effectively. The main reason for such a trend is high frequent occurrence of empty DRX for higher $\Pr(\mathcal{H}_0)$.

TABLE III
ACHIEVED VALUES OF POWER SAVING PARAMETER η AS A FUNCTION OF DRX PARAMETERS, TRAFFIC TYPE, AND SNR PER BIT, ASSUMING THAT $X = 4,\ M = 8,$ AND $\nu = -0.4$

Traffic	on-duration	inactivity	$\Pr(\mathcal{H}_0)$	E_b/N_0	η
VoIP	2	4	60%	-10 dB	42%
VoIP	2	4	60%	0 dB	59%
VoIP	2	4	60%	10 dB	62%
Video	4	4	70%	-10 dB	40%
Video	4	4	70%	0 dB	64%
Video	4	4	70%	10 dB	68%
Data	10	10	70%	-10 dB	43%
Data	10	10	70%	0 dB	66%
Data	10	10	70%	10 dB	70%

VIII. CONCLUSION

In this paper, methods to reduce power consumption of DRX-enabled mobile devices during receive mode without degrading the user experience were pursued. Novel PGM signaling approach was proposed together with an efficient signal structure, such that reliable PGM detection, and thus large energy savings can be obtained in 5G and beyond UE receivers. PGM detection performance was quantified analytically, while it was also shown through link-level simulations that the proposed approach is able to reduce the power consumption of DRX, by up to 70%, 68% and 62% for bursty data applications, video streaming and VoIP, respectively. Our future work will focus on developing a prototype implementation of the proposed PGM signaling concept.

REFERENCES

[1] F. Boccardi, R. W. Heath, A. Lozano, T. L. Marzetta, and P. Popovski, "Five disruptive technology directions for 5G," *IEEE Communications Magazine*, vol. 52, no. 2, pp. 74–80, February 2014.

[2] "Designing mobile devices for low power and thermal efficiency," Qualcomm Technologies Technologies, Inc., Tech. Rep., Oct. 2013.

[3] M. Lauridsen, "Studies on mobile terminal energy consumption for LTE and future 5G," Ph.D. dissertation, Aalborg University, Jan. 2015.

[4] A. Carroll and G. Heiser, "An analysis of power consumption in a smartphone," in *Proc. USENIXATC2010*. Berkeley, CA, USA: USENIX Association, 2010, pp. 21–21.

[5] M. Lauridsen, P. Mogensen, and T. B. Sorensen, "Estimation of a 10 gb/s 5G receiver's performance and power evolution towards 2030," in *Proc. IEEE VTC 2015 Fall*, Sept 2015, pp. 1–5.

[6] J. Huang, F. Qian, A. Gerber, Z. M. Mao, S. Sen, and O. Spatscheck, "A close examination of performance and power characteristics of 4G LTE networks," in *Proc. ACM MobiSys 2012*. New York, NY, USA: ACM, 2012, pp. 225–238.

[7] E. Dahlman, S. Parkvall, and J. Skold, *4G: LTE/LTE-Advanced for Mobile Broadband*. Elsevier Science, 2011.

[8] S. Varma R, K. M. Sivalingam, L.-P. Tung, and Y.-D. Lin, "Dynamic DRX algorithms for reduced energy consumption and delay in LTE networks," in *2014 IFIP Wireless Days (WD)*, Nov 2014, pp. 1–8.

[9] M. Stojanovic, J. G. Proakis, and J. A. Catipovic, "Analysis of the impact of channel estimation errors on the performance of a decision-feedback equalizer in fading multipath channels," *IEEE Transactions on Communications*, vol. 43, no. 2/3/4, pp. 877–886, Feb 1995.

[10] A. Ferrante, N. Laurenti, C. Masiero, M. Pavon, and S. Tomasin, "On the error region for channel estimation-based physical layer authentication over rayleigh fading," *IEEE Transactions on Information Forensics and Security*, vol. 10, no. 5, pp. 941–952, May 2015.

[11] J. G. Proakis and D. K. Manolakis, *Digital Signal Processing (4th Edition)*, 4th ed. Prentice Hall, Apr. 2006.

[12] I. Kuon and J. Rose, "Measuring the gap between FPGAs and ASICs," *IEEE Transactions on Computer-Aided Design of Integrated Circuits and Systems*, vol. 26, no. 2, pp. 203–215, Feb 2007.

[13] T. Kolding, J. Wigard, and L. Dalsgaard, "Balancing power saving and single user experience with discontinuous reception in LTE," in *Proc. IEEE ISWCS 2008*, Oct 2008, pp. 713–717.

[14] C. C. Tseng, H. C. Wang, F. C. Kuo, K. C. Ting, H. H. Chen, and G. Y. Chen, "Delay and power consumption in LTE/LTE-A DRX mechanism with mixed short and long cycles," *IEEE Transactions on Vehicular Technology*, vol. 65, no. 3, pp. 1721–1734, March 2016.

[15] W. A. Khan, "Impact of DRX on VoIP performance and battery life in LTE," Master's thesis, Blekinge Institute of Technology, Jan. 2009.